Oh, B.-H., & Markley, J. L. (1989) *Biopolymers 28*, 1833-1837.
Oh, B.-H., & Markley, J. L. (1990) *Biochemistry* (third paper of three in this issue).
Oh, B.-H., Westler, M. W., Darba, P., & Markley, J. L. (1988) *Science 240*, 908-911.
Oh, B.-H., Westler, W. M., Markley, J. L. (1989) *J. Am. Chem. Soc. 111*, 3083-3085.
Oh, B.-H., Mooberry, E. S., & Markley, J. L. (1990) *Biochemistry* (second paper of three in this issue).
Phillips, W. D., & Poe, M. (1973) in *Iron Sulfur Proteins* (Lovenberg, W., Ed.) Vol. II, pp 255-284, Academic Press, New York and London.
Poe, M., Phillips, W. D., Glickson, J. D., McDonald, C. C., & San Pietro, A. (1971) *Proc. Natl. Acad. Sci. U.S.A. 68*, 68-71.
Rance, M., Sørensen, O. W., Bodenhausen, G., Wagner, G., Ernst, R. R., & Wüthrich, K. (1983) *Biochem. Biophys. Res. Commun. 117*, 479-485.
Salmeen, I., & Palmer, G. (1972) *Arch. Biochem. Biophys. 150*, 767-773.
Shaka, A. J., Keeler, J., Frenkiel, T., & Freeman, R. (1983) *J. Magn. Reson. 52*, 335-338.
Shon, K., & Opella, S. J. (1989) *J. Magn. Reson. 82*, 193-197.
Stockman, B. J., Westler, W. M., Darba, P., & Markley, J. L. (1988a) *J. Am. Chem. Soc. 110*, 4095-4096.
Stockman, B. J., Westler, W. M., Mooberry, E. S., & Markley, J. L. (1988b) *Biochemistry 27*, 136-142.
Stockman, B. J., Reily, M. D., Westler, W. M., Ulrich, E. L., & Markley, J. L. (1989) *Biochemistry 28*, 230-236.
Trebst, A., & Avron, M., Eds. (1977) *Photosynthesis*, Vol. I, Photosynthetic Electron Transport and Photophosphorylation, Springer-Verlag, New York.
Tsukihara, T., Fukuyama, K., Nakamura, M., Katsube, Y., Tanaka, N., Kakudo, M., Wada, K., Hase, T., & Matsubara, H. (1981) *J. Biochem. 90*, 1763-1773.
Tsukihara, T., Fukuyama, K., & Katsube, Y. (1986) in *Iron-Sulfur Protein Research* (Matsubara, H., et al., Eds.) pp 59-68, Japan Science Society Press, Tokyo.
Tsutusi, T., Tsukihara, T., Fukuyama, K., Katsube, Y., Hase, T., Matsubara, H., Nishikawa, Y., & Tanaka, N. (1983) *J. Biochem. 94*, 299-302.
Westler, W. M., Kainosho, M., Nagao, H., Tomonaga, N., & Markley, J. L. (1988) *J. Am. Chem. Soc. 110*, 4093-4095.
Wüthrich, K. (1986) *NMR of Proteins and Nucleic Acids*, pp 130-161, Wiley, New York.

Multinuclear Magnetic Resonance Studies of the 2Fe·2S* Ferredoxin from *Anabaena* Species Strain PCC 7120. 2. Sequence-Specific Carbon-13 and Nitrogen-15 Resonance Assignments of the Oxidized Form†

Byung-Ha Oh, Eddie S. Mooberry, and John L. Markley*

Department of Biochemistry, College of Agricultural and Life Sciences, University of Wisconsin—Madison, 420 Henry Mall, Madison, Wisconsin 53706

Received October 19, 1989

ABSTRACT: Multinuclear two-dimensional NMR techniques were used to assign nearly all diamagnetic ^{13}C and ^{15}N resonances of the plant-type 2Fe·2S* ferredoxin from *Anabaena* sp. strain PCC 7120. Since a ^{13}C spin system directed strategy had been used to identify the ^{1}H spin systems [Oh, B.-H., Westler, W. M., & Markley, J. L. (1989) *J. Am. Chem. Soc. 111*, 3083-3085], the sequence-specific ^{1}H assignments [Oh, B.-H., & Markley, J. L. (1990) *Biochemistry* (first paper of three in this issue)] also provided sequence-specific ^{13}C assignments. Several resonances from ^{1}H–^{13}C groups were assigned independently of the ^{1}H assignments by considering the distances between these nuclei and the paramagnetic 2Fe·2S* center. A ^{13}C–^{15}N correlation data set was used to assign additional carbonyl carbons and to analyze overlapping regions of the ^{13}C–^{13}C correlation spectrum. Sequence-specific assignments of backbone and side-chain nitrogens were based on ^{1}H–^{15}N and ^{13}C–^{15}N correlations obtained from various two-dimensional NMR experiments.

Until recently, extensive assignments in NMR[1] spectra of proteins have been confined to protons, and the wealth of information provided by ^{13}C and ^{15}N nuclei was largely neglected. Although sequence-specific ^{1}H resonance assignments are available for about 60 small proteins [for a review, see Markley (1989)], extensive ^{13}C assignments are limited to only three proteins: bovine pancreatic trypsin inhibitor (Wagner & Brühwiler, 1986), turkey ovomucoid third domain (Robertson et al., 1989), and staphylococcal nuclease (Wang et al., 1990). Extensive backbone nitrogen assignments are limited to bovine pancreatic trypsin inhibitor (Glushka & Cowburn, 1987), staphylococcal nuclease (Torchia et al., 1989; Wang et al., 1990), inflammatory protein C5a (Zuiderweg & Fesik, 1989), DNA binding protein Ner from phage Mu (Gronen-

† This work was supported by USDA Competitive Grant 88-37262-3406 and National Institutes of Health Grant RR02301 from the Biomedical Research Technology Program, Division of Research Resources, and made use of the National Magnetic Resonance Facility at Madison, which is supported in part by Grant RR023021. Additional equipment in the facility was purchased with funds from the University of Wisconsin, the NSF Biological Biomedical Research Technology Program (Grant DMB-8415048), the NIH Shared Instrumentation Program (Grant RR02781), and the U.S. Department of Agriculture. B.-H.O. is supported by a Peterson Fellowship from the University of Wisconsin—Madison.

* To whom correspondence should be addressed.

[1] Abbreviations used are defined in Oh and Markley (1990a).

0006-2960/90/0429-4004$02.50/0

born et al., 1989a), and T4 lysozyme (F. W. Dahlquist, personal communication).

Although ^1H-detected heteronuclear chemical shift correlation experiments have been carried out with concentrated protein samples at natural isotopic abundance (Bax et al., 1983; Westler et al., 1984; Ortiz-Polo et al., 1986; Wagner & Brühwiler, 1986), the low natural abundances of ^{13}C (1.1%) and ^{15}N (0.4%) has prevented the full exploitation of the single-bond and multiple-bond scalar couplings present in protein spin systems. Uniform or selective ^{13}C and/or ^{15}N isotope enrichment can be used to increase the sensitivity of hetero- and homonuclear chemical shift correlation experiments. It is now widely accepted that isotope-aided NMR spectroscopy of enriched protein samples facilitates resonance assignments. In addition to heteronuclear single-bond correlation experiments (Griffey & Redfield, 1987), many powerful 2D NMR experiments have been proposed recently that provide useful additional chemical shift correlations: ^{13}C–^{13}C correlation (Oh et al., 1988; Oh & Markley, 1989; Stockman et al., 1988; Westler et al., 1988a), ^{13}C–^{15}N correlation (Westler et al., 1988b; Mooberry et al., 1989; Niemczura et al., 1989), multiple-bond ^1H–^{13}C or ^1H–^{15}N correlation (Bax & Summers, 1986; Bax & Marion, 1988; Clore et al., 1988; Stockman et al., 1989), long-range heteronuclear ^1H–^{13}C or ^1H–^{15}N correlation (Brühwiler & Wagner, 1986; Lerner & Bax, 1986; Clore et al., 1988; Torchia et al., 1989; Oh et al., 1989; Wang et al., 1990), and ^1H–^{15}N correlation with NOE relay (Shon et al., 1989; Gronenborn et al., 1989b; Wang et al., 1990). In addition, heteronuclear 3D NMR experiments have been reported that spread out two-dimensional ^1H–^1H correlations over the ^{13}C or ^{15}N chemical shift range (Fesik & Zuiderweg, 1989; Fesik et al., 1989; Bax et al., 1989; Zuiderweg & Fesik, 1989).

Isotope-aided 2D and 3D NMR experiments [see Stockman and Markley (1989) for a recent review] not only have paved the way toward resonance assignments of larger proteins (M_r > 10000) but also provide additional ways of studying protein structure, function, and dynamics. These include (1) detailed descriptions of internal motions in proteins based on ^{13}C relaxation measurements (McCain et al., 1988; Nirmala & Wagner, 1988) or 2D exchange spectroscopy (Montelione & Wagner, 1989), (2) refinement of solution structures by use of dihedral angles measured from heteronuclear multiple-bond coupling constants (Montelione et al., 1989; Kay et al., 1989), by identification of more NOE cross peaks than can be assigned from ^1H NOESY data alone, or by use of isotope-edited NOESY data (Shon et al., 1989; Gronenborn et al., 1989b), and (3) determination of the pK_a values of ionizable groups on the basis of the pH dependence of carbon chemical shifts (Grissom & Markley, 1989).

In this paper, we describe the 2D NMR strategies that led to nearly complete sequence-specific resonance assignments of ^{13}C and ^{15}N atoms in the diamagnetic part of oxidized *Anabaena* 7120 ferredoxin on the basis of the sequence-specific ^1H resonance assignments of the protein (Oh & Markley, 1990a). These assignments have assisted in deducing the overall folding of the protein in solution and in characterizing the hyperfine-shifed ^{15}N resonances of the ferredoxin (Oh & Markley, 1990b).

Materials and Methods

Isotope Enrichment and Protein Purification. [26% U-^{13}C]Ferredoxin or [98% U-^{15}N]ferredoxin was produced, respectively, by growing the *Anabaena* 7120 on 26% $^{13}CO_2$ as its sole carbon source or $K^{15}NO_3$ (98+ atom %) as its sole nitrogen source. Double-labeled [26% U-^{13}C,98% U-^{15}N]-ferredoxin was produced by growing the cyanobacterium on 26% $^{13}CO_2$ and $K^{15}NO_3$ (98+ atom %) as its sole carbon and nitrogen sources. Additional experimental details are given in Oh and Markley (1990a).

Chemicals. Sources of isotopes were the Mound Facility of the Monsanto Research Corp. for $K^{15}NO_3$ and Isotec, Inc., for $^{13}CO_2$ (99+ atom %). The $^{13}CO_2$ was diluted with natural abundance CO_2 to 26 atom % ^{13}C and mixed with air to 10% total CO_2. Other chemicals were of reagent grade or better.

NMR Spectroscopy. NMR sample preparations were similar to those described in Oh and Markley (1990a). The $^1H\{^{13}C\}$ SBC, $^1H\{^{15}N\}$ SBC, and $^1H\{^{15}N\}$ MBC spectra were obtained on a Bruker AM-500 (11.7 T) NMR spectrometer with a Bruker 5-mm inverse broad-band probe by employing Bruker reverse electronics with or without WALTZ-16 X-nucleus decoupling (Shaka et al., 1983) during acquisition to collapse heteronuclear couplings.

The $^{13}C\{^{13}C\}$ DQC spectrum was collected on a Bruker AM-500 NMR spectrometer equipped with a Bruker 5-mm broad-band probe. The 90° carbon pulse width was 7.5 μs. The delay time for the double-quantum propagator was set at 10 ms to optimize for one-bond ^{13}C–^{13}C couplings (~50 Hz). WALTZ-16 ^1H decoupling was used during acquisition to collapse ^1H–^{13}C splitting.

The $^{13}C\{^{15}N\}$ SBC spectrum (Mooberry et al., 1989) was obtained on the Bruker AM-400 wide-bore NMR spectrometer with a special Bruker 10-mm quadruple-tuned probe for ^{13}C (observe), ^1H, ^{15}N, and ^2H (lock). WALTZ-16 (Shaka et al., 1983) ^1H decoupling was employed during acquisition to collapse ^1H–^{13}C and ^1H–^{15}N splittings.

The ^1H chemical shifts are referenced to internal TSP. The ^{15}N chemical shifts are referenced to liquid ammonia; the resonance of [^{15}N]ammonium sulfate used as the external standard was taken to be 21.6 ppm at 25 °C. The ^{13}C chemical shifts are referenced to external tetramethylsilane; the dioxane signal, which was an external standard, was taken to be 67.8 ppm at 25 °C.

Results

Carbon Assignment Strategy. Conventionally, protonated ^{13}C nuclei have been assigned by ^1H–^{13}C correlations [as reviewed in Griffey and Redfield (1987)] on the basis of ^1H resonances previously assigned. However, with these data alone, overlap and crowding of ^1H resonances hinder extensive cross assignments of ^{13}C nuclei. This problem can be overcome partially by experiments that correlate ^1H and ^{13}C nuclei separated by more than one bond (Oh et al., 1990a; Lerner & Bax, 1986; Wagner & Brühwiler, 1986). Since the magnitudes of relayed coherences are dependent on three-bond ^1H coupling constants, unfavorable dihedral angles can lead to missing relay cross peaks. This feature limits the extent of ^{13}C assignments by this approach, especially for methylene carbons, which fall in the most crowded spectral region. The $^{13}C\{^{13}C\}$ DQC experiment, which exploits direct, one-bond, ^{13}C–^{13}C coupling, provides cross peaks from all pairs of directly bonded carbon atoms. The much greater chemical shift dispersion of ^{13}C resonances, as compared to ^1H resonances, makes the ^{13}C–^{13}C correlation experiment the most reliable way of assigning side-chain carbons, including quaternary carbons that do not have attached protons.

α-Carbon Assignments. The $^1H\{^{13}C\}$ SBC data (Figure 1) permitted the extension of $^1H^\alpha$ resonance assignments (Oh & Markley, 1990a) to $^{13}C^\alpha$ resonances. Fifty-one cross peaks from $^{13}C^\alpha$–$^1H^\alpha$ units had been previously linked to corresponding $^1H^\alpha$,H^N cross peaks in the COSY fingerprint region by means of a $^1H\{^{13}C\}$ SBC-HH experiment (Oh et al., 1989).

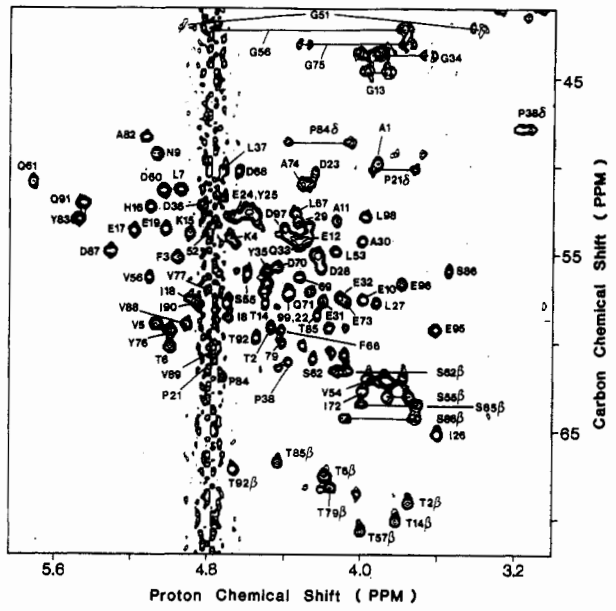

FIGURE 1: Selected region of the 500-MHz $^1H\{^{13}C\}$ SBC spectrum of oxidized [26% U-^{13}C]ferredoxin from *Anabaena* 7120. The sample consisted of 0.5 mL of 7.0 mM ferredoxin in ^2H_2O containing 50 mM phosphate buffer at pH* 7.5. 512 blocks of FID's were collected as 4096 data points; each represented the average of 32 transients. A delay time of 3.57 ms was chosen to optimize for 140-Hz ^1H–^{13}C couplings. Assignments are designated by the one-letter code for amino acids followed by residue position in the amino acid sequence. In crowded regions, only the residue numbers are given.

Thus, those $^{13}C^{\alpha}$ resonances could be assigned according to the sequence-specific $^1H^{\alpha}$ assignments. The remaining $^1H^{\alpha}$ assignments were then transferred to unassigned $^1H^{\alpha}$,$^{13}C^{\alpha}$ cross peaks by chemical shift comparison.

Side-Chain Carbon Assignments. The specific $^{13}C^{\alpha}$ assignments then were extended to corresponding $^{13}C^{\alpha}$,$^{13}C^{\alpha+\beta}$ cross peaks in the $^{13}C\{^{13}C\}$ DQC map through the use of $^1H\{^{13}C\}$ SBC-HH data (Oh et al., 1989). Sequence-specific assignments of side-chain carbons were obtained by following the previously determined ^{13}C–^{13}C connectivities (Oh et al., 1988) starting from α-carbons. Figure 2 shows five examples of sequence-specific assignments of side-chain carbons achieved by following ^{13}C–^{13}C connectivities in the $^{13}C\{^{13}C\}$ DQC spectrum. Aromatic carbons, including nonprotonated carbons, were assigned (Figure 8) primarily from $^{13}C\{^{13}C\}$ DQC data.

The $^1H\{^{13}C\}$ SBC data were used to correlate $^1H^{\gamma}$–$^{13}C^{\gamma}$ and $^1H^{\gamma'}$–$^{13}C^{\gamma'}$ of valine residues and $^1H^{\delta}$–$^{13}C^{\delta}$ and $^1H^{\delta'}$–$^{13}C^{\delta'}$ of isoleucine residues. The $^{13}C^{\zeta}$ of the single arginine (Arg^{42}) was observed in the 1D ^{13}C spectrum and was assigned on the basis of its characteristic chemical shift position [data are not presented here, but virtually the same spectrum is in Chan and Markley (1983b)].

Backbone Carbonyl Carbon Assignments. In principle, backbone carbonyl carbons can be assigned by tracing $^{13}C^{\alpha}$–$^{13}C'$ connectivities. However, this region of the $^{13}C\{^{13}C\}$ DQC spectrum is the most crowded because of the similarity of the $^{13}C^{\alpha}$ and $^{13}C'$ chemical shifts from different residues. Thus, with $^{13}C\{^{13}C\}$ DQC data alone, $^{13}C'$ resonance assignments proved difficult. The $^{13}C\{^{15}N\}$ experiment (Figure 3), which disperses the carbonyl carbon resonances over the amide nitrogen chemical shift range, permitted the correlation of backbone $^{13}C'_i$ and $^{15}N_{i+1}$ resonances. Figure 3 shows sequence-specific assignments of 39 of the backbone $^{13}C'$ resonances on the basis of ^{15}N assignments (see below) or $^{13}C^{\alpha}$–$^{13}C'$ connectivities.

Nitrogen Assignment Strategy. In the 1D ^{15}N NMR spectrum of a diamagnetic protein, the backbone resonances from the amino terminus and Pro and the side-chain resonances from His, Trp, Arg, and Lys occur in distinctive chemical shift regions (Witanowski et al., 1981) so that they can be distinguished easily and assigned to residue types. For a sequence-specific assignment, however, one needs to collect ^1H–^{15}N single-bond or multiple-bond correlation data. The signals from amide nitrogens (peptide bonds and the side chains of Gln and Asn) generally overlap within a 40 ppm region centered around 120 ppm. Heteronuclear single-bond or multiple-bond correlation experiments provide the methods of choice for resolving and analyzing the amide region.

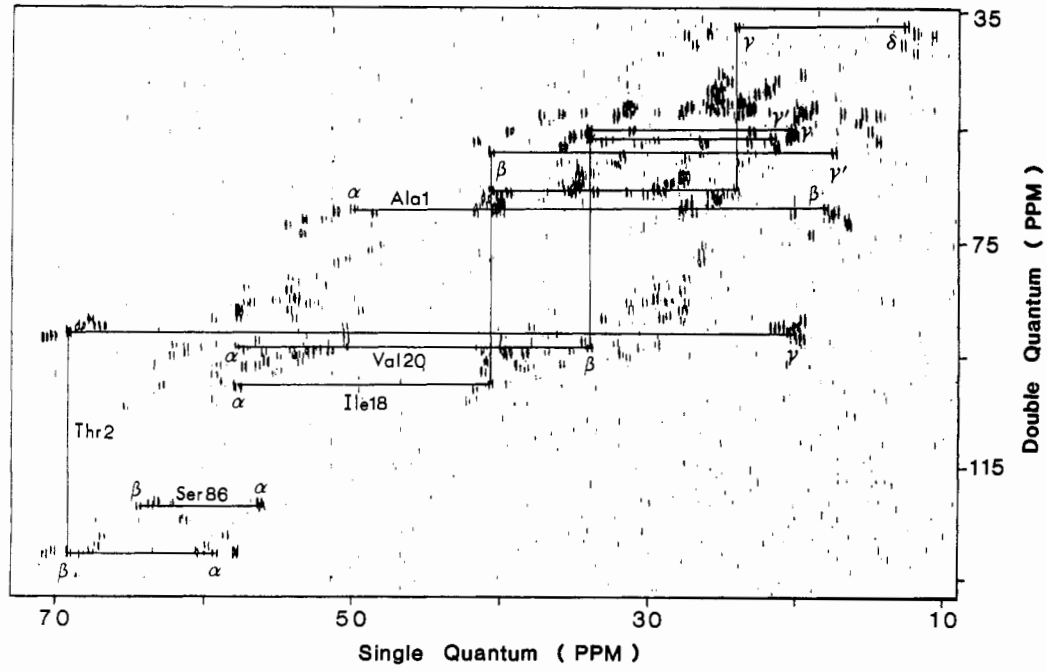

FIGURE 2: Representative regions of the 125-MHz $^{13}C\{^{13}C\}$ DQC spectrum of oxidized [26% U-^{13}C]ferredoxin from *Anabaena* 7120. Solid lines show how carbon assignments were traced from the α-carbons to the terminal side-chain carbons by means of ^{13}C–^{13}C connectivities. Sample preparation and conditions for the NMR experiment were reported previously (Oh et al., 1989).

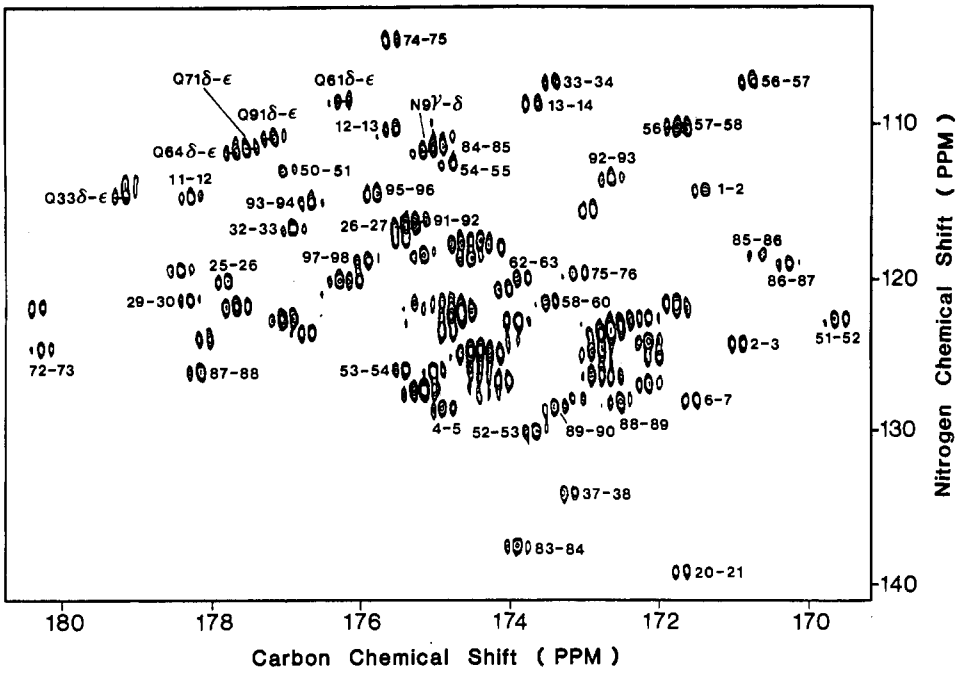

FIGURE 3: $^{13}C\{^{15}N\}$ SBC spectrum (100.6 MHz ^{13}C, 40.55 MHz ^{15}N) of oxidized *Anabaena* 7120 ferredoxin. The sample was 4.5 mM [26% U-^{13}C,95% U-^{15}N]ferredoxin in 2.2 mL of 40 mM phosphate buffer containing 90% ^1H_2O/10% ^2H_2O; the pH of the sample was 7.1. A total of 128 FID blocks were collected as 8192 data points; each represented the average of 1024 transients. The experiment time was 38 h. In the labeling scheme used, X–Z represents a $^{13}C'$,^{15}N cross peak from a dipeptide unit where X and Z stand for residue i and $i + 1$, respectively. The intraresidue $^{13}C^{\delta}$,$^{15}N^{\epsilon}$ and $^{13}C^{\gamma}$,$^{15}N^{\delta}$ cross peaks of Gln and Asn also are indicated.

Backbone Amide Nitrogens. Figure 4 shows the $^1H\{^{15}N\}$ SBC map of *Anabaena* 7120 ferredoxin recorded in 90% ^1H_2O/10% ^2H_2O. Many cross-peak assignments could be based on $^1H^N$ assignments (Oh & Markley, 1990a). However, overlaps of $^1H^N$ resonances led to ambiguous assignments in the $^1H\{^{15}N\}$ SBC map. We overcame this problem by exploiting differences in amide proton exchange rates. The $^1H\{^{15}N\}$ SBC spectrum recorded in ^2H_2O was compared directly with the ^1H COSY spectrum also recorded in ^2H_2O (Figure 5). This comparison provided assignments of the amide groups that remained unexchanged. The exchange-labile amide groups were assigned subsequently, mostly by elimination on comparison of the $^1H\{^{15}N\}$ SBC and ^1H COSY data recorded in ^1H_2O with the data of Figure 5. Remaining ambiguities were removed by identifying NOE relay cross peaks between pairs of direct amide cross peaks in the $^1H\{^{15}N\}$ SBC-NOE spectrum (Oh & Markley, 1990a; Figure 4); the NOE relay cross peaks can be compared with $^1H\{^1H\}$ NOESY data. In Figure 4, one weakly observed cross peak (enclosed by a rectangle) was not assigned. Its corresponding ^{15}N signal was identified in the 1D ^{15}N NMR spectrum (Oh & Markley, 1990b; Figure 1).

Aliphatic Side-Chain Nitrogens. The side-chain nitrogens of all Asn (1) and Gln (5) residues were accounted for by resonances resolved in the $^1H\{^{15}N\}$ SBC spectrum (Figure 4). The side-chain amide ($-NH_2$) groups of Asn and Gln exhibit pairs of cross peaks in the $^1H\{^{15}N\}$ SBC spectrum that serve to distinguish them from the single peaks of backbone amide ($-NH-$) groups. Assignments of these nitrogens were based on the $^{13}C\{^{15}N\}$ SBC data (Figure 3) by extension of the side-chain carbonyl carbon assignments.

The $^{15}N^{\zeta}$ signals of the four lysines in the ferredoxin were resolved and assigned by means of a $^1H\{^{15}N\}$ MBC experiment. Figure 6 compares the 1D ^{15}N NMR spectrum with two-bond $^{15}N^{\zeta}$–$^1H^{\epsilon}$ and three-bond $^{15}N^{\zeta}$–$^1H^{\delta}$ connectivities of the four lysines identified in the $^1H\{^{15}N\}$ MBC spectrum. Since the $^{15}N^{\zeta}$,$^1H^{\delta}$ cross peaks overlapped, the nitrogen assignments

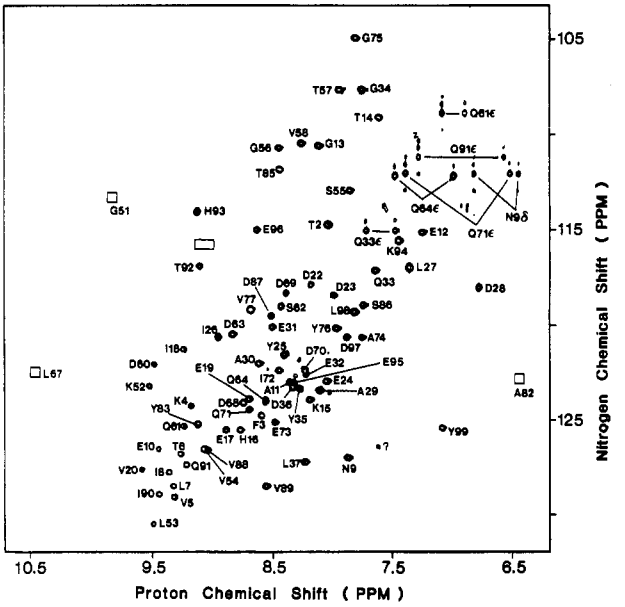

FIGURE 4: $^1H\{^{15}N\}$ SBC spectrum (500 MHz ^1H, 50.68 MHz ^{15}N) of oxidized *Anabaena* 7120 ferredoxin. The sample consisted of 0.5 mL of 6.5 mM [95% U-^{15}N]ferredoxin in 90% ^1H_2O/10% ^2H_2O containing 50 mM phosphate buffer at pH 7.1. The spectrum was recorded with ^{15}N decoupling during acquisition; as a result, the cross peaks appear as singlets. A jump and return pulse sequence (Plateau, & Guéron, 1982) was used for solvent suppression. The square boxes indicate cross peaks that were lost by this solvent-suppression scheme. Cross peaks were observed at these positions when water-peak irradiation was used for solvent suppression (Figure 7). The rectangular box indicates the position of a cross peak visible only at lower contour levels. The spectral width in the ^{15}N dimension was set to the minimum value (64.78 ppm). 450 FID blocks were collected as 4096 data points; each represented the average of 72 transients. The experiment time was 16 h. The labeling scheme for assigned cross peaks is the same as in Figure 1. The weak peak labeled "?" was assigned tentatively to Ser^{65}.

derived from the lysine $^1H^{\epsilon}$ assignments (Oh & Markley, 1990a). Lys^{52} did not show any multiple-bond ^1H–^{15}N cross

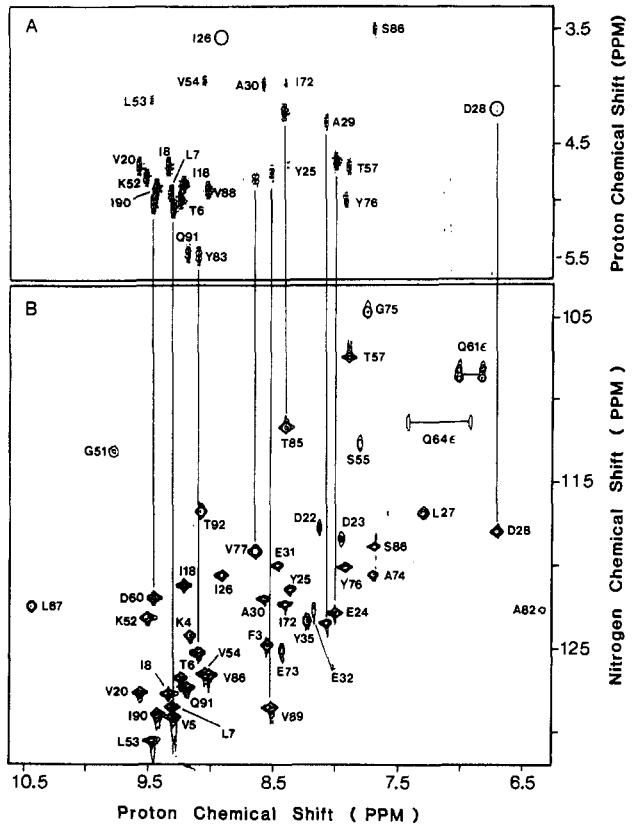

FIGURE 5: Two-dimensional (A) ^1H COSY spectrum (600 MHz) and (B) $^1H\{^{15}N\}$ SBC (500 MHz ^1H, 50.68 MHz ^{15}N) of oxidized *Anabaena* 7120 ferredoxin recorded in ^2H_2O. The sample for spectrum A consisted of 0.5 mL of 9 mM ferredoxin dissolved in ^2H_2O containing 50 mM phosphate buffer at pH* 7.5. The sample for spectrum B was the same as that described in Figure 4 except that the protein was dissolved in ^2H_2O. 512 blocks of FID's were collected as 4096 data points; each represented the average of 104 transients for (A) or 12 transients for (B). The $^1H\{^{15}N\}$ SBC spectrum, which was recorded 8 h following sample preparation, contains more cross peaks than the ^1H COSY spectrum, which was recorded about 48 h after sample preparation.

peaks, but it could be assigned by elimination. The $^{15}N^{\zeta},^1H^{\epsilon}$ cross peaks are weaker than the $^{15}N^{\zeta},^1H^{\delta}$ cross peaks, as expected, since $^2J_{N-H}$ is smaller than $^3J_{N-H}$ (Bystrov, 1976).

^{15}N NMR signals from the one $^{15}N^{\epsilon}$ and two $^{15}N^{\eta}$ of the single arginine (Arg^{42}) were assigned in the 1D ^{15}N NMR spectrum (Oh & Markley, 1990b; Figure 1) on the basis of chemical shift considerations (Witanowski et al., 1981). In the crystal structure, Arg^{42} is located on the loop that tightly surrounds the paramagnetic 2Fe·2S* center, and the side chain of Arg^{42} points away from the 2Fe·2S* center (Tsukihara et al., 1981). The coupling connectivities for Arg^{42} are totally missing in the COSY spectrum, owing to paramagnetic broadening; however, its side-chain nitrogens are observed. The weak Arg^{42} $^1H^{\epsilon}$–$^{15}N^{\epsilon}$ single-bond cross peak also was observed in the $^1H\{^{15}H\}$ SBC spectrum (Figure 7).

Histidine Ring Nitrogens. We used the $^1H\{^{15}N\}$ SBC experiment (Figure 7) to elucidate the combined $^{15}N,^1H$ spin systems of the two histidine residues. The $^1H\{^{15}N\}$ SBC 2D spectrum normally contains cross peaks only from one-bond coupling ($^1J_{NH}$ = 90 Hz for amide ^{15}N–^1H). With the imidazole rings of histidine, however, because the multiple-bond coupling constants are fairly large ($^2J_{N^{\epsilon 2}-H^{\epsilon 1}} = -10.2$, $^2J_{N^{\delta 1}-H^{\epsilon 1}} = -8.2$, $^2J_{N^{\epsilon 2}-H^{\delta 2}} = -5.9$, and $^3J_{N^{\delta 1}-H^{\delta 2}} = -1.8$ at pH 7.6; Blomberg & Rüterjans, 1983), we found cross peaks corresponding to two- or three-bond coupling. The cross-peak intensities (Figure 7), which reflect the magnitudes of the coupling constants between the correlated ^1H and ^{15}N atoms, were used to provide assignments to particular nitrogens and hydrogens. The most intense cross peaks were assigned to $^2J_{N^{\epsilon 2}-H^{\epsilon 1}}$ correlations, which exhibit the largest coupling constant. A cross peak corresponding to the $^3J_{N^{\delta 1}-H^{\delta 2}}$ interaction (smallest coupling constant) is missing in each rectangle (Figure 7). Assignment of the combined $^{15}N,^1H$ spin systems to individual histidines (His^{16} and His^{93}) was accomplished by comparing these connectivities to the sequence-specific imidazole ^1H assignments (Oh & Markley, 1990a).

Proline and Amino-Terminus Nitrogens. The ^{15}N resonances from the three prolines (Pro^{21}, Pro^{38}, and Pro^{84}) were assigned, two from the $^{13}C'$ resonance assignments of their respective preceding residues (Val^{20}, Leu^{37}) by ^{13}C–^{15}N correlations (Figure 3) and the third by elimination on the basis of its characteristic chemical shift. The proline identification based on chemical shift were confirmed by noting the longer

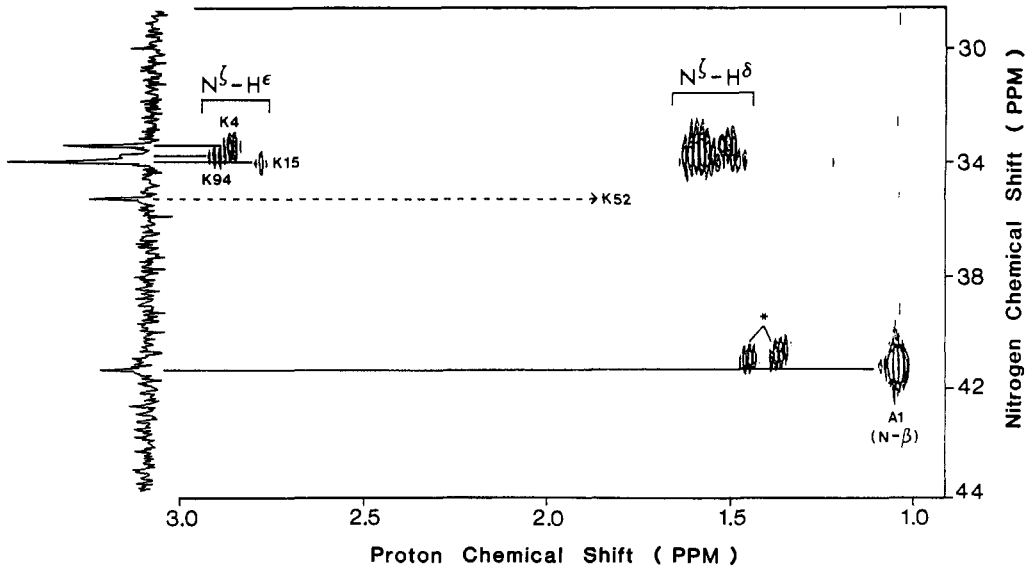

FIGURE 6: $^1H\{^{15}N\}$ MBC spectrum (500 MHz ^1H, 50.68 MHz ^{15}N) of oxidized *Anabaena* 7120 ferredoxin. The sample was the same as that described in Figure 5B. The delay time was set 70 ms to optimize for 7-Hz multiple-bond ^1H–^{15}N couplings. Positive and negative components of peaks are plotted without distinction. The 1D ^{15}N spectrum displayed over the ^{15}N chemical shift axis is the one described in Figure 1 of the following paper (Oh & Markley, 1990b). The spectrum contains two spurious cross peaks labeled with asterisks (*) that line up at a common ^{15}N chemical shift; since no ^{15}N signal was detected at this chemical shift in the 1D ^{15}N spectrum, they appear to be artifacts.

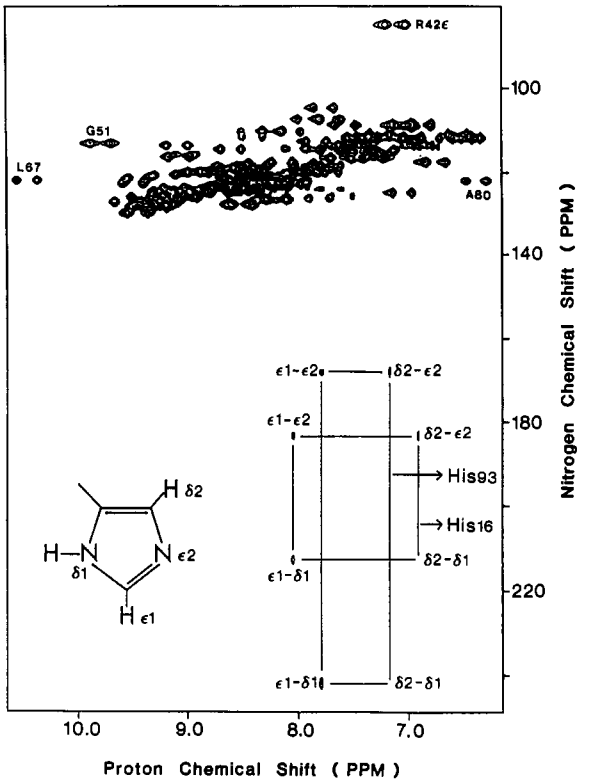

FIGURE 7: $^1H\{^{15}N\}$ SBC spectrum (500 MHz ^1H, 50.68 MHz ^{15}N) of oxidized *Anabaena* 7120 ferredoxin. The spectral width in the ^{15}N dimension was 259.11 ppm, which included all downfield ^{15}N resonances. The sample was the same as that described in Figure 4. The spectrum was recorded without ^{15}N decoupling during acquisition; as a result, the cross peaks appear as doublets. Solvent suppression was achieved by irradiation at the solvent frequency during the relaxation delay (1.2 s). Cross peaks in the upper part of the spectrum represent single-bond ^1H–^{15}N correlations. The cross peaks assigned to Gly[51], Leu[67], and Ala[82], which were not observed in Figure 4, are labeled. Cross peaks representing multiple-bond ^1H–^{15}N connectivities in the histidine ring are labeled according to the nomenclature shown in the inset. For clarity, only one tautomeric form of the neutral imidazole ring of histidine is shown. A total of 480 FID blocks were collected as 4096 data points; each represented the average of 80 transients. The experiment time was 18 h.

spin–lattice relaxation times (T_1) of the three Pro ^{15}N signals (due to the absence of a proton on the proline nitrogen) as compared to those of the other amide nitrogens (Oh & Markley, 1990b). In principle, the proline ^{15}N also can be assigned from $^1H\{^{15}N\}$ MBC data. However, the ^{15}N signals of the three prolines did not show any multiple-bond cross peaks (data not shown).

The ^{15}N resonance from the amino terminus of a protein usually falls in the lysine $^{15}N^{\zeta}$ region and may be difficult to distinguish from the lysine signals on the basis of a 1D spectrum. In the present case, the ^{15}N signal of Ala[1] was identified cleanly by a cross peak in the $^1H\{^{15}N\}$ MBC spectrum (Figure 6), which was attributed to a three-bond connectivitiy between the alanine $^1H^{\beta}$ and ^{15}N.

Assignments to Residues Affected by Paramagnetic Interactions. In the ^1H COSY experiment, cross-peak intensities are proportional to the homonuclear two- or three-bond coupling constant; the three-bond coupling varies between 0 and 16 Hz depending on the dihedral angle. Thus, one cannot observe all possible cross peaks from three-bond scalar-coupled proton pairs. For a small diamagnetic protein, the missing peaks usually can be reconstituted from NOESY data since NOE cross peaks from vicinal protons are strong in cases when the corresponding COSY peaks are weak. In larger proteins or paramagnetic proteins, however, such cross peaks often are missing in NOESY spectra particularly when the relaxation times of resonating nuclei are shorter than the NOESY mixing time.

Table I: Distances (Å) between the Two Iron Atoms of the 2Fe·2S* Center and the Carbon Atoms of Those Amino Acids Whose ^1H Spin Systems Were Totally Absent or Only Partly Observed in $^1H\{^1H\}$ 2D Spectra[a]

residue		distance[b] Fe1	Fe2	residue		distance[b] Fe1	Fe2
Ala[43]	C^{α}	5.69	5.80	Ser[47]	C^{α}	5.91	5.79
	C^{β}	6.71	7.17		C^{β}	7.35	7.36
Ala[45]	C^{α}	5.98	7.00	Ser[65]	C^{α}	12.99	11.34
	C^{β}	6.65	8.02		C^{β}	12.73	11.14
Ala[50]	C^{α}	8.56	6.57	Thr[48]	C^{α}	5.86	5.92
	C^{β}	9.00	7.18		C^{β}	5.79	6.46
Leu[27]	C^{α}	11.34	9.62		C^{γ}	4.60	10.67
	C^{β}	9.89	8.30	Thr[79]	C^{α}	9.54	7.05
Leu[78]	C^{α}	8.88	6.40		C^{β}	10.30	7.93
	C^{β}	8.78	6.41		C^{γ}	5.78	8.29
Phe[39][c]	C^{β}	6.15	6.10	Val[81]	C^{α}	9.98	7.93
	C^{γ}	7.29	7.50		C^{β}	9.86	7.94
Phe[66]	C^{β}	10.23	8.78		C^{γ}	8.68	7.01
	C^{γ}	10.78	9.50		$C^{\gamma'}$	10.08	8.01

[a] Distances are presented only for carbon atoms that are candidates for cross peaks observed in the $^{13}C\{^{13}C\}$ DQC spectrum. [b] Distances were calculated from the coordinates of *Spirulina platensis* ferredoxin (Tsukihara et al., 1981). Fe1 is the iron atom that is ligated to Cys[41] and Cys[46]; Fe2 is the iron atom that is ligated to Cys[49] and Cys[80]. [c] Residue 39 in *S. platensis* ferredoxin is tyrosine; it is replaced by phenylalanine in *Anabaena* 7120 ferredoxin. The distances of the C^{β} and C^{γ} of this residue from the iron atoms were assumed to be identical in both proteins.

Heteronuclear single-bond correlation experiments involve coherence-transfer steps that utilize large heteronuclear single-bond couplings ($^1J_{CH}$ = 140–160 Hz and $^1J_{NH}$ = 90 Hz). They allow the detection of ^1H resonances that are too broad to be detected in homonuclear ^1H NMR experiments. More ^{13}C spin systems than ^1H spin systems can be detected since the $^{13}C\{^{13}C\}$ DQC experiment utilizes the large one-bond ^{13}C–^{13}C coupling (~50 Hz) and since the paramagnetic line broadening effect on ^{13}C resonances is 16 times smaller than that on ^1H resonances (for ^1H and ^{13}C nuclei at the same distance from a paramagnetic center; Bloembergen & Morgan, 1961).

In the $^{13}C\{^{13}C\}$ DQC spectrum of oxidized *Anabaena* 7120 ferredoxin, complete or partial ^{13}C–^{13}C connectivities were determined for several residues whose corresponding ^1H spin systems were unobserved or only partly observed in the COSY spectrum; complete carbon spin systems for one each of Ala, Phe, Ser, Thr, Tyr, and Val and incomplete ^{13}C–^{13}C connectivities for one Leu and one Phe. Classification of the ^{13}C spin systems by amino acid type was based on characteristic ^{13}C chemical shifts and ^{13}C–^{13}C connectivity patterns. Their sequence-specific assignments to Tyr[25], Leu[27], Ala[50], Phe[39], Phe[66], Ser[65], Thr[79], and Val[81] were based primarily on the proximity of these residues to the 2Fe·2S* center in the X-ray crystal structure of a related ferredoxin (Tsukihara et al., 1981). These (except for Leu[27]) are the only ^{13}C assignments that were based on the crystal structure of the ferredoxin.

Table I shows the distances from the 2Fe·2S* center of carbon atoms of those residues whose ^1H resonances were not resolved in 2D spectra. Among the three alanines not observed in homonuclear ^1H 2D spectra, Ala[50] is the farthest from the two irons; thus, the unassigned Ala carbon connectivities observed in the $^{13}C\{^{13}C\}$ DQC spectrum were assigned to Ala[50]. Similar arguments were used to assign carbons of Leu[27], Ser[65], and Thr[79]. The Leu[27] assignment was confirmed by the identification of the $^{13}C'$,^{15}N cross peak from the dipeptide

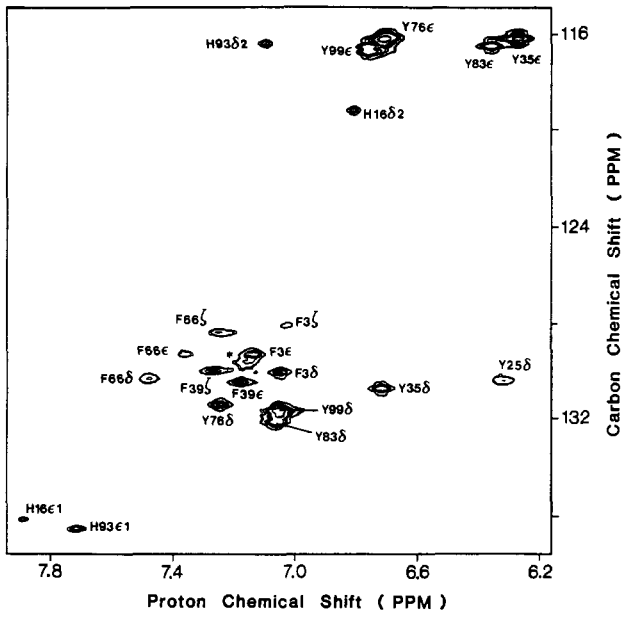

FIGURE 8: Aromatic region of the $^1H\{^{13}C\}$ SBC spectrum of oxidized [26% U-^{13}C]ferredoxin from *Anabaena* 7120. The protein sample and experimental conditions were the same as described in Figure 1, except that the delay time in the pulse sequence was set to 3.13 ms in order to optimize for the 160-Hz aromatic ^1H–^{13}C couplings. The intensity labeled with an asterisk (*) appears to be an artifact since all of the aromatic carbons have been assigned.

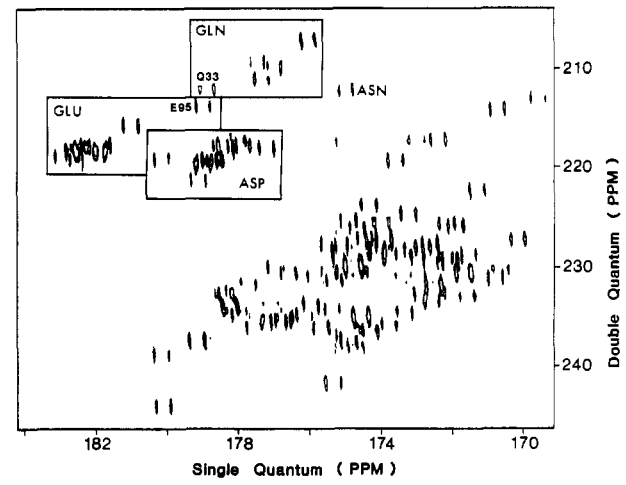

FIGURE 9: Carbonyl carbon region of the $^{13}C\{^{13}C\}$ DQC spectrum of oxidized [26% U-^{13}C]ferredoxin from *Anabaena* 7120 described in Figure 2. The four different types of side-chain carbonyl carbons lie in separated spectral regions. Other peaks represent $^{13}C'$,$^{13}C^{\alpha+\prime}$ cross peaks from the peptide backbone. Positive and negative components of each peak are plotted here without distinction.

Ile^{26}-Leu^{27} in the $^{13}C\{^{15}N\}$ SBC spectrum (Figure 3). Most of the protons attached to the observed carbons of these four amino acids were assigned by the presence of cross peaks in the $^1H\{^{13}C\}$ SBC spectrum (Figure 1). Figure 8 shows assignments in the aromatic region of the $^1H\{^{13}C\}$ SBC spectrum. $^1H^{\alpha}$,$^1H^{N}$ cross peaks from Phe^{39} and Phe^{66} were not observed in COSY and NOESY spectra. Complete ^{13}C–^{13}C connectivities were observed for Phe^{66} in the $^{13}C\{^{13}C\}$ DQC spectrum (data not shown). However, ^{13}C–^{13}C connectivities for only the ring portion of Phe^{39} were observed. The latter connectivities were assigned to Phe^{39} and the former to Phe^{66} on the basis of the fact that Phe^{39} is closer to the 2Fe·2S* center than Phe^{66} (Table I). The T_1 of the $^{13}C^{\gamma}$ assigned to Phe^{39} was six times shorter than that assigned to Phe^{66} (Chan & Markley, 1983). All aromatic carbon assignments were extended to the attached protons (Figure 8) except $^1H^{\delta}$ of Phe^{39}. Its line width must be broadened in comparison with the coupling constant ($>{}^1J_{CH}$). The $^1H^{\delta}$,$^1H^{\epsilon}$ cross peak of Phe^{39} also was not observed in COSY and NOESY spectra. The remaining tyrosine aromatic ^{13}C–^{13}C correlation in the $^{13}C\{^{13}C\}$ DQC spectrum was assigned to Tyr^{25} by elimination, since those of the other four tyrosines were assigned previously. The $^1H^{\delta}$,$^1H^{\epsilon}$ cross peak from Tyr^{25} was not observed in COSY or NOESY spectra.

Discussion

All of the ^{13}C and ^{15}N resonance assignments are summarized, along with ^1H resonance assignments, in Table I of the preceding paper in this series (Oh & Markley, 1990a). We note that the ^{13}C–^{13}C connectivities assigned to Glu and Asp fall in a different chemical shift region from those of Gln and Asn, respectively, in the $^{13}C\{^{13}C\}$ DQC map. The side-chain carboxy carbons of all Glu and Asp resonate well downfield from those of all Gln and Asn, except for Glu^{95} and Gln^{33} (Figure 9). Thus, the environmental contribution to the chemical shifts of side-chain carbonyl carbons appears to be smaller than that of electron shielding. This means that these amino acid types can be distinguished correctly, in most cases, on the basis of their chemical shifts in the $^{13}C\{^{13}C\}$ DQC spectrum alone.

In the past, selective ^{15}N labeling of one of the two nitrogens has been the method of choice for the specific assignments of imidazole ring nitrogens of histidine. This has required laborious organic synthesis. The simple technique for assigning imidazole ring nitrogens presented in this paper appears to have general applicability, since similar characteristic box-shaped ^1H–^{15}N correlation patterns (Figure 7) have been obtained in $^1H\{^{15}N\}$ SBC spectra of three other proteins, flavodoxin and cytochrome *c*-553 from *Anabaena* 7120 (W. M. Westler, B. J. Stockman, and J. L. Markley, unpublished results) and staphylococcal nuclease (A. P. Hinck, S. N. Loh, J. Wang, and J. L. Markley, unpublished results). Although multiple-bond ^1H–^{15}N connectivities of the imidazole ring of a histidine also can be determined by the $^1H\{^{15}N\}$ MBC experiment, such data do not provide the characteristic differences in peak intensities needed to assess the magnitudes of multiple-bond coupling constants and allow specific ^{15}N assignments.

The assignments presented in this paper and the preceding paper (Oh & Markley, 1990a) provide the foundation for future studies of the structure, dynamics, and molecular interactions of this protein. The analysis of interproton distances will be greatly aided by $^1H\{^{13}C\}$ SBC-NOE and $^1H\{^{15}N\}$ SBC-NOE data since both ^{13}C and ^{15}N are assigned. Homo- and heteronuclear coupling constant measurements, the latter obtained with labeled samples, will provide additional constraints for refining the three-dimensional structure. In addition, the assigned ^{13}C and ^{15}N resonances can serve as reporters of interactions between the ferredoxin and its redox partners.

Acknowledgments

We thank Dr. W. M. Westler for assistance and helpful discussions.

References

Bax, A., & Summers, M. F. (1986) *J. Am. Chem. Soc. 108*, 2093–2094.

Bax, A., & Marion, D. (1988) *J. Magn. Reson. 78*, 186–191.

Bax, A., Griffey, R. H., & Hawkins, B. L. (1983) *J. Magn. Reson. 55*, 301–315.

Bax, A., Kay, L. E., Sparks, S. W., & Torchia, D. A. (1989) *J. Am. Chem. Soc. 111*, 408–409.
Blomberg, F., & Rüterjans, H. (1983) *Biol. Magn. Reson. 5*, 21–73.
Brühwiler, D., & Wagner, G. (1986) *J. Magn. Reson. 69*, 546–551.
Bystrov, V. F. (1976) *Prog. Nucl. Magn. Reson. Spectrosc. 10*, 58–61.
Chan, T.-M., & Markley, J. L. (1983) *Biochemistry 22*, 5996–6002.
Clore, G. M., Bax, A., Wingfield, P., & Gronenborn, A. M. (1988) *FEBS Lett. 238*, 17–21.
Fesik, S. W., & Zuiderweg, E. R. P. (1989) *J. Magn. Reson. 78*, 588–593.
Fesik, S. W., Gampe, R. T., Jr., & Zuiderweg, E. R. P. (1989) *J. Am. Chem. Soc. 111*, 770–772.
Glushka, J., & Cowburn, D. (1987) *J. Am. Chem. Soc. 109*, 7879–7881.
Griffey, R. H., & Redfield, A. G. (1987) *Q. Rev. Biophys. 19*, 51–82.
Grissom, C. A., & Markley, J. L. (1989) *Biochemistry 28*, 2116–2124.
Gronenborn, A. M., Bax, A., Wingfield, P. T., & Clore, G. M. (1989a) *Biochemistry 28*, 5081–5089.
Gronenborn, A. M., Bax, A., Wingfield, P. T., & Clore, G. M. (1989b) *FEBS Lett. 243*, 93–98.
Kay, L. E., Brooks, B., Sparks, S. W., Torchia, D. A., & Bax, A. (1989) *J. Am. Chem. Soc. 111*, 5488–5490.
Lerner, L., & Bax, A. (1986) *J. Magn. Reson. 69*, 375–380.
Markley, J. L. (1989) *Methods Enzymol. 176*, 12–64.
McCain, D. C., Ulrich, E. L., & Markley, J. L. (1988) *J. Magn. Reson. 80*, 296–305.
Montelione, G. T., & Wagner, G. (1989) *J. Am. Chem. Soc. 111*, 3096–3098.
Montelione, G. T., Winkler, M. E., Rauenbuehler, P., & Wagner, G. (1989) *J. Magn. Reson. 82*, 198–204.
Mooberry, E. S., Oh, B.-H., & Markley, J. L. (1989) *J. Magn. Reson. 85*, 147–149.
Niemczura, W. P., Helms, G. L., Chesnick, A. S., Moore, R. E., & Bornemann, V. (1989) *J. Magn. Reson. 81*, 635–640.
Nirmala, N. R., & Wagner, G. (1988) *J. Am. Chem. Soc. 110*, 7557–7558.
Oh, B.-H., & Markley, J. L. (1989) *Biopolymers 28*, 1833–1837.
Oh, B.-H., & Markley, J. L. (1990a) *Biochemistry* (first paper of three in this issue).
Oh, B.-H., & Markley, J. L. (1990b) *Biochemistry* (third paper of three in this issue).
Oh, B.-H., Westler, M. W., Darba, P., & Markley, J. L. (1988) *Science 240*, 908–911.
Oh, B.-H., Westler, W. M., & Markley, J. L. (1989) *J. Am. Chem. Soc. 111*, 3083–3085.
Ortiz-Polo, G., Krishnamoorthi, R., Markley, J. L., Live, D. H., Davis, D. G., & Cowburn, D. (1986) *J. Magn. Reson. 68*, 303–310.
Plateau, P., & Guéron, M. (1982) *J. Am. Chem. Soc. 104*, 7310–7311.
Robertson, A. D., Rhyu, G. I., Westler, W. M., & Markley, J. L. (1989) *Biopolymers* (in press).
Shaka, A. J., Keeler, J., Frenkiel, T., & Freeman, R. (1983) *J. Magn. Reson. 52*, 335–338.
Shon, K., & Opella, S. J. (1989) *J. Magn. Reson. 82*, 193–197.
Stockman, B. J., & Markley, J. L. (1989) in *Advances in Biophysical Chemistry* (Bush, C. A., Ed.) Vol. 1, JAI Press, Greenwich, CT (in press).
Stockman, B. J., Reily, M. D., Westler, W. M., Ulrich, E. L., & Markley, J. L. (1989) *Biochemistry 28*, 230–236.
Torchia, D. A., Sparks, S. W., & Bax, A. (1989) *Biochemistry 28*, 5509–5524.
Tsukihara, T., Fukuyama, K., Nakamura, M., Katsube, Y., Tanaka, N., Kakudo, M., Wada, K., Hase, T., & Matsubara, H. (1981) *J. Biochem. 90*, 1763–1773.
Wagner, G., & Brühwiler, D. (1986) *Biochemistry 25*, 5839–5843.
Wang, J., Hinck, A. P., Loh, S. N., & Markley, J. L. (1990) *Biochemistry 29*, 102–113.
Westler, W. M., Ortiz-Polo, G., & Markley, J. L. (1984) *J. Magn. Reson. 58*, 354–357.
Westler, W. M., Kainosho, M., Nagao, H., Tomonaga, N., & Markley, J. L. (1988a) *J. Am. Chem. Soc. 110*, 4093–4095.
Westler, W. M., Stockman, B. J., Markley, J. L. Hosoya, Y., Miyake, Y., & Kainosho, M. (1988b) *J. Am. Chem. Soc. 110*, 6256–6258.
Witanowski, M., Stefaniak, L., & Webb, G. A. (1981) *Annu. Rep. NMR Spectrosc. 11B*, 1–502.
Zuiderweg, E. R. P., & Fesik, S. W. (1989) *Biochemistry 28*, 2387–2391.